A Link-layer Synchronization and Medium Access Control Protocol for Terahertz-band Communication Networks

Qing Xia*, **Zahed Hossain***, **Michael Medley**† and **Josep Miquel Jornet***

*Department of Electrical Engineering, University at Buffalo, The State University of New York, Buffalo, New York 14260, USA, E-mail: {qingxia, zahedhos, jmjornet}@buffalo.edu

†Air Force Research Laboratory/RITE, Rome, NY 13441, USA, Email: michael.medley@us.af.mil

***Abstract*—In this paper, a link-layer synchronization and medium access control (MAC) protocol for very-high-speed wireless communication networks in the THz band is presented. The protocol relies on a receiver-initiated handshake as a way to guarantee synchronization between transmitter and receiver. In addition, it incorporates a sliding window flow control mechanism, which combined with the one-way handshake, maximizes the channel utilization. Two different application scenarios are considered, namely, a macroscale scenario, in which nodes utilize turning directional antennas to periodically sweep the space while overcoming the distance problem at THz frequencies, and a nanoscale scenario, in which nano-nodes require energy harvesting systems to operate. A carrier-based physical layer is considered for the macro-scenario, whereas the physical layer for the nano-scenario is based on a femtosecond-long pulse-based modulation scheme with frame interleaving. The performance of the proposed MAC protocol is analytically investigated in terms of delay, throughput and successful packet transmission probability, and compared to that of an adapted Carrier Sense Multiple Access with Collision Avoidance with and without handshake. The results are validated by means of extensive simulations with *ns*-3, in which all the necessary THz elements have been implemented. The results show that the proposed protocol can maximize the successful packet delivery probability without compromising the achievable throughput in THz-band communication networks.**

I. Introduction

Over the last decade, wireless data traffic has drastically increased due to a change in the way today's society creates, shares and consumes information. This change has been accompanied by an increasing demand for higher speed wireless communication anywhere, anytime. Following this trend, wireless multi-Gigabit-per-second (Gbps) and Terabit-per-second (Tbps) links are expected to become a reality within the next five to ten years. In this context, Terahertz (THz)-band (0.1–10 THz) communication is envisioned as a key technology to satisfy the need for such very high data-rates, both in traditional networking paradigms as well as in novel nanoscale machine communication networks or nanonetworks [1].

For many years, the lack of compact and efficient ways to generate and detect THz-band signals has limited the feasibility of such communication systems. However, within the last five years, outstanding progress has been achieved towards the development of compact THz-band transceivers and antennas. Different technologies have been considered to date, ranging from Silicon Germanium [2] and compound semiconductor technologies based on III-V semiconductors [3], to photonic devices such as Quantum Cascade Lasers (QCLs) [4] and, more recently, novel nanomaterials such as graphene [5].

The THz band provides wireless communication devices with an unprecedentedly large bandwidth, ranging from several tens of GHz up to a few THz [6], [7]. The main phenomenon affecting the propagation of THz-band signals is the absorption by water vapor molecules. For communication distances below one meter, where the number of molecules found along the path is small, the THz band behaves as a single transmission window several THz wide. On the other hand, for distances beyond a few meters, molecular absorption defines multiple transmission windows, each of them tens or hundreds of GHz wide. In both cases, physical-layer data-rates in the order of hundreds of Gbps and few Tbps have already been demonstrated, even with low-complexity modulations [8].

In parallel to the development of THz devices and physical layer mechanisms, there is a need to investigate new networking solutions for very-high-speed wireless data networks. Traditional Medium Access Control (MAC) protocols need to be revised in light of the properties of THz-band communication. In particular, the THz band provides devices with a very large bandwidth and, thus, these do not need to aggressively contend for the channel. In addition, such very large bandwidth results in very high bit-rates and, consequently, very short transmission times, which further minimize the collision probability.

However, due to the low transmission power of THz transceivers and the high path-loss at THz-band frequencies, very high directivity antennas are needed to establish wireless links beyond one meter. While directional communication further decreases multi-user interference, it requires tight synchronization between transmitter and receiver to overcome the deafness problem [9]. Moreover, the relatively long propagation delay when transmitting at Tbps over multi-meter-long links results in low channel utilization. While these two issues vanish in nanoscale applications, there are other challenges that affect the link layer design of THz nano-devices, such as their temporal energy fluctuations and, thus, availability, introduced by required energy harvesting systems [10].

To overcome these limitations, in this paper, we develop a synchronization and MAC protocol for very-high-speed wireless communication networks in the THz band. The protocol relies on a receiver-initiated handshake as a way to guarantee

Acknowledgement of Support and Disclaimer: (a) The State University of New York at Buffalo acknowledges the U.S. Government's support in the publication of this paper. This material is based upon work funded by AFRL, under AFRL Grant No. FA8750-15-1-0050. (b) Any opinions, findings and conclusions or recommendations expressed in this material are those of the author(s) and do not necessarily reflect the views of AFRL.

Approved for Public Release; Distribution Unlimited: 88ABW-2015-2394.

synchronization between transmitter and receiver. In addition, it incorporates a sliding window flow control mechanism, which combined with the one-way handshake, maximizes the channel utilization. We consider two different application scenarios: a macroscale scenario, in which nodes utilize high-speed turning directional antennas to periodically sweep the space, and a nanoscale scenario, in which nodes make use of a piezoelectric nano-generator to harvest energy. For each scenario, we consider a different physical layer, namely, a traditional carrier-based modulation for the macro-scenario and a femtosecond-long pulse-based modulation with user interleaving for the nano-scenario. We analytically investigate the performance of the proposed MAC protocol in terms of delay, throughput and successful packet transmission probability, and compare it to that of a modified Carrier Sense Multiple Access with Collision Avoidance (CSMA/CA) with and without handshake. In addition, we have implemented in *ns*-3 the proposed protocol and the necessary THz models (channel, carrier-based and pulse-based physical layers, turning antenna and harvesting system), and provide extensive simulation results to validate the performance of our solution.

The remainder of this paper is organized as follows. We summarize the related work in Sec. II. In Sec. III, we describe the system model considered throughout the paper and derive formulations for the bit and frame error rate, the probability of collision in the macroscale and the nanoscale scenarios, and the energy harvesting system for nano-devices. In Sec. IV, we describe the proposed protocol and analytically investigate its performance for the two scenarios. We provide simulation and numerical results in Sec. V and conclude the paper in Sec. VI.

II. Related Work

To the best of our knowledge, there are no existing protocols for macroscale THz-band communication networks. Available solutions for lower-frequency systems cannot directly be utilized in this paradigm, mainly because they do not capture the peculiarities of the THz-band channel or the capabilities of THz devices. In terms of frequency, millimeter-wave (mm-wave) systems [11], such as those at 60 GHz, are the closest existing technology. In addition to the IEEE 802.11ad standard [12], which mainly adopts a very similar link layer to that of the entire IEEE 802.11 family, a few alternative MAC protocols for mm-wave systems have already been developed [13]–[15]. These protocols are mainly aimed at solving the deafness problem introduced by directional antennas. As in many of the directional MAC protocols for lower frequency bands [16], [17], the existing solutions assume that a node can alternate between directional and omnidirectional antenna modes. However, at THz-band frequencies, highly-directional antennas are simultaneously needed both at the transmitter and the receiver to successfully establish the link.

When it comes to nanonetworks, there are not many MAC solutions for the time being. In [18], we proposed the PHLAME, the first MAC protocol for ad-hoc nanonetworks. In this protocol, nano-devices such as nanosensors are able to dynamically choose different physical layer parameters based on the channel conditions and the energy of the nano-devices. Similarly, in [19], we proposed a centralized MAC protocol, in which a nano-controller would determine the best communication parameters for the nano-devices. In both cases, a transmitter-initiated hand-shake was required, which would eventually result into a low channel utilization. In [20], a receiver-initiated MAC protocol for nanosensor networks was proposed. The developed protocol is based on a distributed scheduling scheme, which requires the nodes to perform a distributed edge coloring algorithm. However, due to the very limited computational resources of individual nano-devices, it seems more plausible to leverage the pulse-based physical layer to interleave users in time, rather than performing distributed scheduling algorithms.

III. THz-band Communication System Model

In this section, we summarize the main peculiarities of THz-band communication networks, both for the macroscale and the nanoscale scenarios. In particular, first, we formulate the Signal-to-Noise Ratio (SNR), which is needed for the computation of Bit Error Rate (BER) and Frame Error Rate (FER), starting from an accurate THz-band channel model. Then, we formulate the collision probability in the macroscale scenario, for which we introduce and analyze the impact of utilizing high-speed turning THz directional antennas, as well as in the nanoscale scenario, for which we revise the concept of interleaved pulse-based transmissions [19]. Finally, we introduce the energy harvesting model utilized in nanonetworks.

A. Signal-to-noise Ratio, Bit Error Rate and Frame Error Rate

The propagation of electromagnetic waves at THz-band frequencies is mainly affected by molecular absorption, which results in both molecular absorption loss and molecular absorption noise. In particular, based on the THz-band channel model introduced in [6], the signal power at a distance d from the transmitter, P_r is given by

$$P_r(d) = \int_B S_t(f) \left|H_c(f,d)\right|^2 \left|H_r(f)\right|^2 df, \qquad (1)$$

where S_t is the single-sided power spectral density (p.s.d) of the transmitted signal, B stands for its bandwidth and f refers to frequency. H_c refers to the THz-band channel frequency response, which is given by

$$H_c(f,d) = \left(\frac{c}{4\pi f d}\right) \exp\left(-\frac{k_{abs}(f)\, d}{2}\right), \qquad (2)$$

where c refers to the speed of light and k_{abs} is the molecular absorption coefficient of the medium. This parameter depends on the molecular composition of the transmission medium, i.e., the type and concentration of molecules found in the channel and is computed as in [6]. H_r in (1) refers to the receiver frequency response, which we consider an ideal low-pass filter with bandwidth B, for the time being.

Similarly, the molecular absorption noise power N_r at a distance d from the transmitter, which can be modeled as additive, Gaussian, colored and correlated to the transmitted signal [8], is given by

$$N_r(d) = \int_B \left(S_{N^B}(f) + S_{N^I}(f,d)\right) \left|H_r(f)\right|^2 df, \qquad (3)$$

where it is taken into account that the total molecular absorption noise is contributed by the background atmospheric noise

p.s.d., S_{N^B} and the self-induced noise p.s.d., S_{N^I}, and are computed as described in [8].

The SNR at a distance d from the transmitter can be then obtained dividing (1) by (3). For a given SNR, the BER, P_b, only depends on the modulation technique. In our analysis, we consider two different physical layers:

- In the macroscale scenario, i.e., for distances above a few meters, we consider that nodes transmit a conventional m-PSK modulated signal over a 100-GHz-wide transmission window at 1.05 THz. This is done to overcome the very high molecular absorption loss over long distances [6].
- In the nanoscale scenario, i.e., for distances much below one meter, we consider that nodes transmit by using TS-OOK, a modulation scheme based on the transmission of one-hundred-femtosecond-long pulses by following an on-off keying modulation spread in time [8]. The p.s.d. of such pulses is mainly contained between 0.9 and 4 THz.

Finally, to compute the frame error rate P_p, we consider that a hybrid error control technique based on the combination of low-weight channel codes with ARQ is utilized [21].

B. Collision Probability

The collision probability depends on the application.

1) Macroscale Scenario: In this case, nodes require high-gain directional antennas in transmission and in reception to successfully establish a link. As we already discussed, this results into low multi-user interference, at the cost of high synchronization requirements. To model the multi-user interference, we need to take into account both the spatial distribution of the nodes as well as their temporal activity. In our model, we consider that nodes are randomly distributed in space by following a spatial Poisson process with rate λ_A. The area of influence of an individual node is given by $A(\theta l) = \frac{\theta}{2\pi}\pi l^2 = \frac{\theta}{2} l^2$, where θ is the antenna beam-width in radians and l stands for the maximum transmission distance. Then, the probability of finding i nodes in A is given by

$$P[i \in A(\theta l)] = \frac{(\lambda_A A(\theta l))^i}{i!} e^{-\lambda_A A(\theta l)}. \quad (4)$$

If each node i in A generates new frames at a rate given by $1/\alpha FT$, where α is a constant and FT stands for frame time, the aggregated traffic generated by i nodes is simply $\lambda_T = i/\alpha FT$. Thus, the probability that j out of i nodes are active during a vulnerable time of $2FT$ is given by:

$$P[j \in 2FT] = \frac{(\lambda_T 2FT)^j}{j!} e^{-\lambda_T 2FT}. \quad (5)$$

Finally, the collision probability in the macroscale scenario is:

$$P_c = \sum_{i=1}^{\infty} P[i \in A(\theta l)] \left(1 - P[0 \in 2FT]\right). \quad (6)$$

2) Nanoscale Scenario: In this case, miniature nodes do not require directional antennas, but transmit omnidirectionally. Therefore, the probability of finding i nodes in the area of influence of a node is given by (4) for $\theta = 2\pi$. This results into a much larger number of potentially interfering nodes. Interestingly, however, TS-OOK supports the simultaneous transmission and reception of time-interleaved frames. In this scheme, a logical "0" is transmitted as silence, whereas a logical "1" is transmitted with a pulse. The time between symbols, pulses and silences, T_s is much longer than the pulse duration T_p, $\beta = T_s/T_p \gg 1$.

By considering that each node i in A generates new frames at a rate $1/\alpha FT$, the rate at which new pulses are generated is given by $\lambda_P = ip_1/\alpha T_s$, where p_1 refers to the probability of transmitting a pulse, and is related to the coding weight [21]. Then, the probability of j out of i nodes generate pulses within the vulnerable time $2T_p$ is:

$$P[j \in 2T_p] = \frac{(\lambda_P 2T_p)^j}{j!} e^{-\lambda_P 2T_p}. \quad (7)$$

Finally, if there are n symbols in one frame, the collision probability of one frame in the nanoscale scenario is:

$$P_c = \sum_{i=1}^{\infty} P[i \in A(2\pi l)] \left(1 - P[0 \in 2T_p]^n\right). \quad (8)$$

C. Nano Energy Model

In our analysis, we are interested in computing the frame error probability caused by insufficient energy at the transmitter or at the receiver. For this, we utilize the same methodology as in [22]. Due to space limitations, we only qualitatively describe our methodology, but refer the reader to the original paper for further details. Mainly, the probability mass function (p.m.f.) of the energy stored at the nano-node battery after reaching a steady state depends both on the rate at which energy is harvested and the rate at which energy is consumed. The latter depends on the the new frame generation rate as well as on the expected number of retransmissions. Ultimately, different MAC protocols result into different number of transmissions and, thus, into different p.m.f. for the energy at the nano-battery. With the p.m.f. of the energy, we can calculate the probability of having enough energy at each node. We implement the harvesting model in *ns*-3 and utilize the collected data to estimate the battery p.m.f. used in our numerical results.

IV. Receiver-initiated Synchronization and Medium Access Control Protocol

In this section, we first describe the proposed protocol for THz-band communication. Then, we analytically investigate its performance in terms of successful packet delivery probability, packet delay and throughput.

A. Protocol Overview

In light of the system model described in Sec. III, it is clear that an initial handshake is needed in THz-band communication networks to guarantee link-layer synchronization between the transmitter and the receiver. The objective of such handshake is to prevent unnecessary data transmissions when the receiver is not available, whether because it is not facing the transmitter (macroscale scenario) or because it does not have enough energy to handle a new transmission (nanoscale scenario). The fundamental idea behind the proposed protocol is to reduce the overhead introduced by such handshaking process by having nodes announce their availability to receive data. In other words, the traditional two-way handshake is reduced to a one-way handshake process. Receiver-initiated

MAC protocols have been successfully utilized in other scenarios [16], [17], [20], but the existing solutions cannot directly be utilized in our scenario because of the aforementioned peculiarities of THz-band communication networks.

Besides the one-way handshake, the proposed protocol also makes use of sliding flow control window at the link layer to maximize the channel utilization. In particular, both the delay introduced while waiting for the receiver availability and the relatively long propagation delay when transmitting at multi-Gbps or Tbps over multi-meter distances (macroscale scenario) result in a relative low channel utilization. To overcome such problem, the receiver can specify the time that it will remain facing in the current direction (macroscale scenario) or the amount of data packets willing to accept with its currently available energy (nanoscale scenario).

The basics of the protocol are summarized next. A node can be found in transmitting mode or in receiving mode:

- A node in *transmitting mode (TM)*, i.e., with data to transmit, checks whether a current Clear-To-Send (CTS) frame from the intended receiver has been recently received. We consider that a CTS has an expiration time, which is a parameter value in our system. If not, the node listens to the channel until the reception of a new CTS frame. In the macroscale scenario, we consider that the node in TM points its directional antenna to the receiver. For this, we consider that, at the link layer, the node in TM knows the position of the receiver. This information is provided by the network layer after a discovery process, which remains as future work. In the nanoscale scenario, we consider that nodes utilize omnidirectional antennas.
- A node in *receiving mode (RM)*, i.e., with sufficient resources (e.g., energy or even memory) to handle a new incoming transmission, broadcasts its status by means of a CTS frame. In the macroscale scenario, the node in RM uses a dynamically turning narrow-beam to broadcast CTS frames while sweeping its entire surrounding space. Such electrically-controlled high-speed turning directional antennas can be implemented for example by means of a very large graphene-based plasmonic nano-antenna array [23]. The node in RM mode cannot know in advance who is willing to transmit, which is why it needs to sweep the entire space. The turning speed of beam is a parameter to be optimized in our analysis. In the nanoscale scenario, this information is omnidirectionally transmitted. The CTS frame also contains information on the receiver's current sliding window size.

Upon the reception of a CTS frame, a node in TM mode checks whether it has data for such receiver and the necessary resources. If so, it proceeds with the DATA frame transmission by taking into account also the receiver sliding window size. If the transmission is successful, the node in RM sends a positive acknowledgement (ACK) frame. Otherwise, after a time-out, the node in TM will set a random back-off time, which depends on the number of transmission attempts, and repeats the entire process when done. After successfully receiving a packet, i.e., successfully transmitting a CTS, a DATA and an ACK frames, the node in RM can decide to keep turning, continue to collect more packets, or switch to TM.

A couple of comments regarding *fairness* need to be made. First, as in any triggered reaction protocol, nodes in TM wait a random time after receiving a CTS frame and before sending the DATA frame. In the macroscale scenario, carrier-sense is performed during that time. In the nanoscale scenario, in which a pulsed-based physical layer is used, there is no carrier to sense, but the chances of having a collision are very low (Sec. III). Second, only for the macroscale scenario, it is relevant to note that the node in RM cannot simply stop indefinitely at a node in TM, but it needs to continue "turning". Therefore, we need to guarantee that, within the small span of time that the node in RM is facing the node in TM, the DATA frame can be successfully transmitted. This is possible because nodes are transmitting at multi-Gbps and even Tbps and, thus, only several nanoseconds are usually needed, which is much lower than in existing wireless communication systems and, thus, can be leveraged to effectively never stop turning.

B. Performance Analysis

To analyze the performance of the proposed protocol, we analytically investigate the successful packet delivery probability, the packet delay and the throughput. First, we focus on the macroscale scenario and develop a mathematical framework in detail. Then, we summarize the differences needed to capture the nanoscale scenario peculiarities.

1) Macroscale Scenario: In this case, the main factor affecting the performance of the protocol is the antenna turning speed ω, given in circles-per-second. In particular, we consider that the antenna shifts its direction in discrete steps and, thus, provides coverage to different sectors in different times. We define the sector time or time during which the antenna beam is pointing to a certain direction as $T_{sector} = \theta / (2\pi\omega)$. This limits the maximum number of retransmissions that a node can complete in the current round s. This affects the overall packet delay and throughput, as the node will have to wait for an entire cycle before being able to continue its ongoing transmission in round $s+1$. More specifically, the maximum number of retransmission η_{max} that a node can complete in round s can be calculated as follows

$$\eta_{max}[s] = \min\left\{ \left\lfloor \frac{T_{sector} - T_{CTS} - T_{prop}}{T_{t/o} + T_{b/o}} \right\rfloor, k[s] \right\}, \quad (9)$$

where $T_{t/o} = 2T_{prop} + T_{proc} + T_{DATA} + T_{ACK}$ is the time-out time, T_{CTS}, T_{DATA} and T_{ACK} refer to the CTS, DATA, and ACK frames transmission time, respectively, and $T_{b/o}$ is a random exponential back-off time. In our analysis, we do not ignore the impact of the propagation delay T_{prop}, as it is comparable or even larger than the frame transmission time in the macroscale scenario. k is a parameter value that specifies the maximum number of retransmissions available in the current round. In particular, $k[1]$ is set to a default value k_0. For example, if $k_0 = 5$, the total amount of retransmissions for a specific packet is equal to 5. This can be "consumed" within one round if T_{sector} is very long, i.e., the antenna turns at a slow speed, or might be spread across rounds, otherwise.

Then, the probability to succeed with exactly i retransmissions within the same round is given by

$$P_{succ}^{i-rtx} = P_{CTS}\left(1 - P_{DATA}P_{ACK}\right)^{i-1} P_{DATA}P_{ACK}, \quad (10)$$

where $P_{CTS} = \overline{P_p} = (1 - P_p)$ is the probability of successfully receiving a CTS frame; $P_{DATA} = \overline{P_c}\ \overline{P_p}$ is the probability of successfully receiving a DATA frame; $P_{ACK} = \overline{P_p}$ is the probability of successfully receiving an ACK frame. We consider that the main reason for not properly receiving the CTS is the presence of bit errors, rather than the collision with other CTS. In the macroscale scenario, this is generally true, as it is very unlikely to have two or more receivers exactly pointing towards the same transmitter with their directional beams. Similarly, in the nanoscale scenario, given the energy constraints of nano-nodes, it is not likely to have many nearby receivers announcing their availability at the same time. When it comes to the DATA frame, failures might occur because of both bit errors as well as collisions. Even if we introduce a random initial delay between the CTS reception and the DATA transmission, collisions can occur. Finally, ACK frames might also suffer from bit errors.

From this, we can easily write the probability to successfully transmit the packet P_{succ}^{rnd} in round s as well as the expected number of retransmissions η in that round as

$$P_{succ}^{rnd}[s] = \sum_{i=1}^{\eta_{max}[s]} P_{succ}^{i-rtx}; \quad \eta[s] = \sum_{i=1}^{\eta_{max}[s]} iP_{succ}^{i-rtx}. \tag{11}$$

If successful, the average successful packet delay introduced by the current round s can be calculated as

$$T_{succ}[s] = (\eta[s] - 1)\left(T_{t/o} + T_{b/o}\right) + T_{succ}^{1}, \tag{12}$$

where $T_{succ}^{1} = 2T_{prop} + T_{proc} + T_{DATA} + T_{ACK}$ is the delay when successfully transmitting the packet in one attempt.

If the node is not successful in the current round, but the maximum number of retransmissions across rounds k_0 has not been yet achieved, the node waits for a new CTS frame (after one antenna cycle). Now $k[s+1] = k[s] - \eta^{max}[s]$. The maximum number of rounds Γ_{max} is given by

$$\Gamma_{max} = \min_{s}\{k[s] = 0\}. \tag{13}$$

Then, the probability to successfully transmit a packet in the j-th round is given by

$$P_{succ}^{j-rnd} = \left(\prod_{u=1}^{j-1}\left(1 - P_{succ}^{rnd}[u]\right)\right) P_{succ}^{rnd}[j], \tag{14}$$

where P_{succ}^{rnd} is given in (11).

From this, the total packet successful delivery probability and the average number of rounds needed to do so are given by

$$P_{succ} = \sum_{j=1}^{\Gamma_{max}} P_{succ}^{j-rnd}; \quad \Gamma = \sum_{j=1}^{\Gamma_{max}} jP_{succ}^{j-rnd}. \tag{15}$$

The discard probability immediately follows as $P_{dis} = \overline{P_{succ}}$. The average packet delay can similarly be obtained as:

$$\begin{aligned} T_{packet} = \sum_{j=1}^{\Gamma_{max}} \prod_{u=1}^{j-1}\left(1 - P_{succ}^{rnd}[u]\right) P_{succ}[j] \\ \cdot\left((j-1)T_{cycle} + T_{succ}[j]\right) + T_{wait}, \end{aligned} \tag{16}$$

where T_{cycle} is the time needed for the antenna to complete one entire circle. T_{wait} refers to the average time that the transmitter will have to wait for the receiver's CTS in the first round, and is computed as follows

$$T_{wait} = \sum_{i=1}^{n_{sectors}} \overline{P_f}^{(i-1)} P_f\,(i-1)\,T_{sector}, \tag{17}$$

where $n_{sectors} = 2\pi/\theta$ is the number of sectors and $P_f = \theta/\pi$ is the transmitter and receiver facing probability. Finally, we can obtain the throughput as $S = n_{packet}/T_{packet}$, where n_{packet} is the number of bits per packet.

2) Nanoscale Scenario: In this case, the main problem affecting the performance of the protocol is posed by the fluctuations in the available energy in each nano-device, which were discussed in Sec. III-C. In our analysis, we consider that the battery in each nano-node can hold up to ϵ_{max} energy frames. An energy frame is the energy in Joules consumed in the reception of a control frame (CTS or ACK), also denoted as $\epsilon_{control}^{rx}$. Similarly, $\epsilon_{control}^{tx}$ denotes the energy frames required to transmit a control frame, and ϵ_{DATA}^{tx} and ϵ_{DATA}^{rx} are the number of energy frames needed to transmit and receive a DATA frame, respectively. The rate at which energy frames are harvested is denoted by λ_{harv}. Based on the probability distribution of the battery energy status, we can calculate the insufficient energy probability and its impact on the system.

The model now is fundamentally the same, with only few modifications. In this case, the reception of a CTS frame is not governed by the antenna turning speed ω and the sector time T_{sector}, but by the time needed by the receiver to harvest enough energy to operate and the announced CTS lifetime. Upon the reception of a CTS frame, the transmitter node checks whether it has enough energy to successfully transmit one or more packets. The new maximum number of retransmissions η_{max} in round s is given by

$$\begin{aligned} \eta_{max}[s] = \min\left\{\left\lfloor\frac{CTS_{life}}{T_{t/o} + T_{b/o}}\right\rfloor, k[s],\right. \\ \left.\left\lfloor\sum_{i=\epsilon^{tx}}^{\epsilon_{max}} P[level = i]\left\lfloor\frac{i - \epsilon^{tx}}{\epsilon_{retry}}\right\rfloor + 1\right\rfloor\right\}, \end{aligned} \tag{18}$$

where CTS_{life} refers to the CTS frame lifetime, set by the receiver according to its energy, $T_{t/o}$ and $T_{b/o}$ are the time-out and back-off times, respectively, defined similarly as for the macroscale scenario, $\epsilon^{tx} = \epsilon_{CTS}^{rx} + \epsilon_{DATA}^{tx} + \epsilon_{ACK}^{rx}$ is the energy required to complete a packet transmission on the transmitter side, $level$ is the number of energy frame units contained in the battery, and ϵ_{retry} is the energy spent in a retransmission. As before, k is a parameter value that specifies the maximum number of retransmissions still available.

In general, there is no guarantee that the transmitter and the receiver will have enough energy to successfully complete the packet transaction in one round, i.e., during the duration of the current CTS lifetime. As a result, both nodes might have to wait to harvest the required energy. The average waiting times for the transmitter and the receiver nodes are given by

$$T_{wait}^{tx/rx} = \frac{1}{\lambda_{harv}} \sum_{i=0}^{\epsilon^{tx/rx}} P[level = i]\left(\epsilon^{tx/rx} - i\right), \tag{19}$$

where $\epsilon^{rx} = \epsilon_{CTS}^{tx} + \epsilon_{DATA}^{rx} + \epsilon_{ACK}^{tx}$ is the required energy to start transmission from receiver side, and λ_{harv} is the energy

harvesting rate in frames per second. Thus, the average waiting time for the packet transmission can be calculated as:

$$T_{wait} = P^{tx}_{wait}\overline{P^{rx}_{wait}}T^{tx}_{wait} + \overline{P^{tx}_{wait}}P^{rx}_{wait}T^{rx}_{wait} + P^{tx}_{wait}P^{rx}_{wait}\max\left\{T^{tx}_{wait}, T^{rx}_{wait}\right\}, \quad (20)$$

where

$$P^{tx}_{wait} = \sum_{i=0}^{\epsilon^{tx}} P\left[level = i\right]; \; P^{rx}_{wait} = \sum_{i=0}^{\epsilon^{rx}} P\left[level = i\right], \quad (21)$$

are the waiting probability for the transmitter and the receiver, respectively. The packet delay T_{delay} can be now obtained by utilizing (20) in (16) instead of (17). The rest of the analytical model remains the same.

V. Numerical and Simulation Results

In this section, we investigate the performance of the proposed protocol and compare it to that of CSMA/CA with and without RTS/CTS (2-way and 0-way handshake). The numerical results obtained by solving the analytical models developed in Sec. IV are validated by simulation obtained with *ns*-3. For this, we have implemented the frequency-selective THz-band channel, the two THz physical layers (carrier-based and pulse-based with interleaving), the high-speed turning antenna, the energy harvesting unit, our proposed protocol and we also tailored and tuned CSMA/CA to work with the THz models. For completeness, we have also developed the analytical models for CSMA/CA with and without RTS/CTS, but these are not included due to space constraints.

A. Macroscale Scenario

In this case, we utilize the following parameter values. The network is composed by 18 nodes over a circular area with radius $l = 10$ m. The transmission power of each node is limited to 10 μW. Nodes are equipped with turning directional antennas with directivity $D = 35$ dB, which corresponds to an antenna beam-width of approximately 32°. The center frequency f_c and bandwidth B are 1.05 THz and 100 GHz, respectively, which corresponds to the first absorption-defined transmission window above 1 THz (any other transmission window can be selected). The antenna turning speed is a parameter in our analysis. The back-off time $t_{b/o}$ and the sector time T_{sector}, which is utilized to also set the receiver sliding window, is adjusted according to the turning antenna speed. The maximum number of retransmissions k_0 is set to 5.

In Fig. 1, the packet discard probability is shown as a function of the antenna turning speed. As expected, with our proposed receiver-initiated or 1-way handshake protocol, the probability of discarding a packet is virtually zero and significantly much lower than 0-way and 2-way protocols. The main reason for this is that no retransmission attempts will be "wasted" when the receiver is not facing the transmitter, i.e., unless the transmitter has recently received a CTS frame from the intended receiver. This is not the case for the two traditional protocols, which might discard up to 30% of their generated packets as the facing probability given in (17) is very low for such very high directivity antennas.

However, the cost of a lower discard probability is reflected in the achievable throughput, which is plotted in Fig. 2 as a function of the antenna turning speed. For low turning antenna speeds, the throughput achieved by 0-way or 2-way protocols is higher than that of the proposed protocol, mainly because, successful packets (less than 80% of the total) have been transmitted when the receiver has been found facing at the transmitter, without the need to wait for it. As the antenna turning speed increases, the throughput for the proposed protocol increases and ultimately meets that of the other two protocols with the advantage of having no packets dropped. The values considered for the turning speed are conservative in light of the theoretically achievable with the aforementioned structures [23].

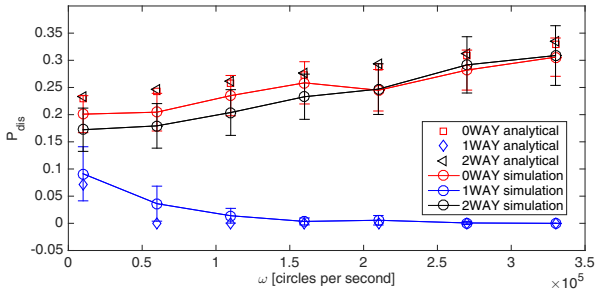

Fig. 1. Discard probability as a function of the antenna turning speed ω.

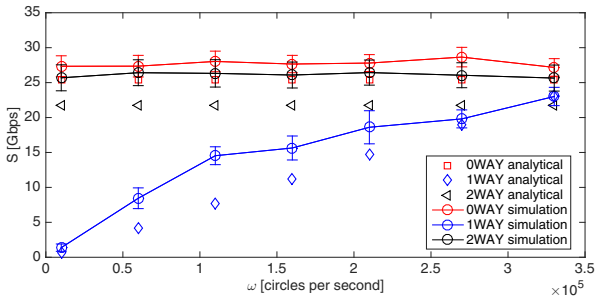

Fig. 2. Throughput as a function of the antenna turning speed ω.

B. Nanoscale Scenario

In this case, we utilize the following parameter values. A circular area with radius $l = 0.01$ m with varying nano-node densities is considered. Nano-nodes communicate by utilizing TS-OOK with pulse energy E_p=1 attoJoule (aJ), pulse length T_p=100 fs, and spreading factor $T_s/T_p = 100$. Nodes utilize omnidirectional antennas with no directivity gain. For the energy model, we define $1/\lambda_{harv} = 8$ μs per energy frame, $\epsilon^{rx}_{control}$=1, $\epsilon^{tx}_{control}$=4, ϵ^{rx}_{DATA}=16, and ϵ^{tx}_{DATA}=64 energy units. The capacity of the battery is ϵ_{max}=1000 energy frames. These values have been obtained by taking into account the energy to transmit and receive a pulse, the coding weight, and the harvesting model given in [22].

In Fig. 3, the packet discard probability is shown as a function of the node density. Similarly as for the macroscale scenario, the number of dropped packets is significantly lower than with the other protocols. It is relevant to note that in this case, the 0-way handshake protocol has also a very low discard probability. The reason for this is because the time needed to harvest energy to transmit a packet is much larger than the time needed to harvest energy to receive. As a result, when

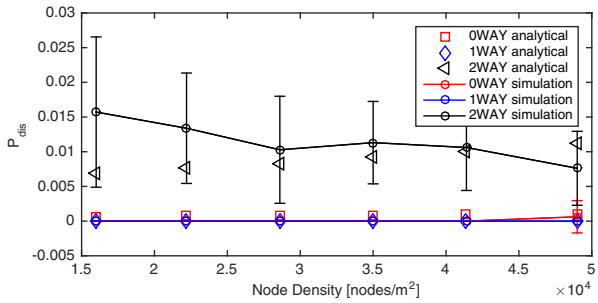

Fig. 3. Packet discard probability as a function of the node density.

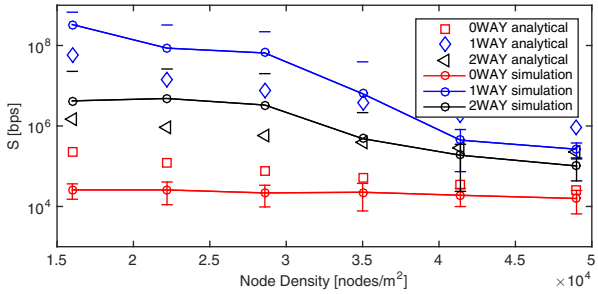

Fig. 4. Throughput as a function of the node density.

the transmitter has enough energy to transmit, it is likely that the receiver has it too. However, for every transmission missed, the time before the next retransmission is very high. This can be seen in Fig. 4, where the throughput is shown as a function of the node density. Note that in this case the throughput for our proposed protocol is significantly higher than for the other two protocols (note the logarithmic scale). The reason is again related to the very long time needed for a node to have enough energy to transmit after a failed transmission. This emphasizes the need for transmitter-receiver synchronization, which is the main reason behind the one-way handshake.

VI. Conclusion

In this paper, we have presented a link-layer synchronization and MAC protocol for ultra-high-speed wireless communication networks in the THz band. The protocol relies on a receiver-initiated handshake as well as a sliding window flow control mechanism to guarantee synchronization between transmitter and receiver, maximize the channel utilization and minimize the packet discard probability. The performance of the proposed protocol is analytically investigated, compared to that of a modified CSMA/CA with and without RTS/CTS, and validated though extensive simulations with *ns*-3. The results show that the proposed protocol can maximize the successful packet delivery probability and enhance the achievable throughput in THz-band communication networks.

References

[1] I. F. Akyildiz, J. M. Jornet, and C. Han, "Terahertz band: Next frontier for wireless communications," *Physical Communication (Elsevier) Journal*, vol. 12, pp. 16 – 32, Sep. 2014.

[2] E. Ojefors, J. Grzyb, B. Heinemann, B. Tillack, and U. R. Pfeiffer, "A 820GHz SiGe chipset for terahertz active imaging applications," in *Proc. of IEEE International Solid-State Circuits Conference*, 2011.

[3] K. Shinohara, D. Regan, Y. Tang, A. Corrion, D. Brown, J. Wong, J. Robinson, H. Fung, A. Schmitz, T. Oh, S. Kim, P. Chen, R. Nagele, A. Margomenos, and M. Micovic, "Scaling of GaN HEMTs and Schottky Diodes for Submillimeter-Wave MMIC Applications," *IEEE Transactions on Electron Devices*, vol. 60, no. 10, pp. 2982–2996, 2013.

[4] Q. Y. Lu, N. Bandyopadhyay, S. Slivken, Y. Bai, and M. Razeghi, "Widely tuned room temperature terahertz quantum cascade laser sources based on difference-frequency generation," *Applied Physics Letters*, vol. 101, no. 25, p. 251121, 2012.

[5] J. M. Jornet and I. F. Akyildiz, "Graphene-based plasmonic nano-antenna for terahertz band communication in nanonetworks," *IEEE JSAC, Special Issue on Emerging Technologies for Communications*, vol. 12, no. 12, pp. 685–694, Dec. 2013.

[6] ——, "Channel modeling and capacity analysis of electromagnetic wireless nanonetworks in the terahertz band," *IEEE Transactions on Wireless Communications*, vol. 10, no. 10, pp. 3211–3221, Oct. 2011.

[7] S. Priebe and T. Kurner, "Stochastic modeling of thz indoor radio channels," *IEEE Transactions on Wireless Communications*, vol. 12, no. 9, pp. 4445–4455, 2013.

[8] J. M. Jornet and I. F. Akyildiz, "Femtosecond-long pulse-based modulation for terahertz band communication in nanonetworks," *IEEE Transactions on Communications*, vol. 62, no. 5, pp. 1742 – 1754, May 2014.

[9] S. Singh, R. Mudumbai, and U. Madhow, "Interference analysis for highly directional 60-ghz mesh networks: The case for rethinking medium access control," *IEEE/ACM Transactions on Networking*, vol. 19, no. 5, pp. 1513–1527, 2011.

[10] P. Bai, G. Zhu, Y. Liu, J. Chen, Q. Jing, W. Yang, J. Ma, G. Zhang, and Z. L. Wang, "Cylindrical rotating triboelectric nanogenerator," *ACS nano*, vol. 7, no. 7, pp. 6361–6366, 2013.

[11] T. Rappaport, J. Murdock, and F. Gutierrez, "State of the art in 60-ghz integrated circuits and systems for wireless communications," *Proceedings of the IEEE*, vol. 99, no. 8, pp. 1390 –1436, Aug. 2011.

[12] *IEEE 802.11ad-2012: Wireless LAN Medium Access Control (MAC) and Physical Layer (PHY) Specifications Amendment 3: Enhancements for Very High Throughput in the 60 GHz Band*, IEEE Standard for Information Technology, Telecommunications and Information Exchange between Systems Std.

[13] T. Tandai, R. Matsuo, T. Tomizawa, H. Kasami, and T. Kobayashi, "Mac efficiency enhancement with prioritized access opportunity exchange protocol for 60 ghz short-range one-to-one communications," in *IEEE 73rd Vehicular Technology Conference (VTC)*, 2011, pp. 1–5.

[14] F. Yildirim and H. Liu, "Directional mac for 60 ghz using polarization diversity extension (dmac-pdx)," in *IEEE Global Telecommunications Conference (GLOBECOM)*, 2007, pp. 4697–4701.

[15] Q. Chen, J. Tang, D. T. C. Wong, X. Peng, and Y. Zhang, "Directional cooperative mac protocol design and performance analysis for ieee 802.11 ad wlans," *IEEE Transactions on Vehicular Technology*, vol. 62, no. 6, pp. 2667–2677, 2013.

[16] R. R. Choudhury, X. Yang, R. Ramanathan, and N. Vaidya, "On designing mac protocols for wireless networks using directional antennas," *IEEE Transactions on Mobile Computing*, vol. 5, no. 5, pp. 477–491, 2006.

[17] M. Takata, M. Bandai, and T. Watanabe, "A receiver-initiated directional mac protocol for handling deafness in ad hoc networks," in *IEEE International Conference on Communications (ICC)*, vol. 9, 2006, pp. 4089–4095.

[18] J. M. Jornet, J. C. Pujol, and J. S. Pareta, "Phlame: A physical layer aware mac protocol for electromagnetic nanonetworks in the terahertz band," *Nano Communication Networks (Elsevier) Journal*, vol. 3, no. 1, pp. 74 – 81, 2012.

[19] P. Wang, J. M. Jornet, M. Abbas Malik, N. Akkari, and I. F. Akyildiz, "Energy and spectrum-aware mac protocol for perpetual wireless nanosensor networks in the terahertz band," *Ad Hoc Networks (Elsevier) Journal*, vol. 11, no. 8, pp. 2541–2555, 2013.

[20] S. Mohrehkesh and M. C. Weigle, "Rih-mac: receiver-initiated harvesting-aware mac for nanonetworks," in *Proceedings of ACM The First Annual International Conference on Nanoscale Computing and Communication*, 2014, pp. 1–9.

[21] J. M. Jornet, "Low-weight error-prevention codes for electromagnetic nanonetworks in the terahertz band," *Nano Communication Networks (Elsevier) Journal*, vol. 5, no. 1-2, pp. 35–44, March-June 2014.

[22] J. M. Jornet and I. F. Akyildiz, "Joint energy harvesting and communication analysis for perpetual wireless nanosensor networks in the terahertz band," *IEEE Transactions on Nanotechnology*, vol. 11, no. 3, pp. 570–580, 2012.

[23] P.-Y. Chen and A. Alù, "Thz beamforming using graphene-based devices," in *IEEE 13th Topical Meeting onSilicon Monolithic Integrated Circuits in RF Systems (SiRF)*, 2013, pp. 36–38.